

Studies of extreme gust storm events in Bengaluru, India

Jyotirmayee Satapathy^{1,*} and G. S. Bhat²

¹Department of Physics, Amrita Vishwa Vidyapeetham, Amritapuri 690 525, India

²Centre for Atmospheric and Oceanic Sciences, Indian Institute of Science, Bengaluru 560 012, India

Many parts of India experience extreme gust and dust storms during the pre-monsoon months of April and May. These events can cause lot of damage to plants and properties. Despite their annual recurrences, their physical nature (e.g. temporal and spatial scales) and mechanism remain unaddressed in the Indian context. Here we present some case studies of pre-monsoon, damage-causing extreme winds reported from Bengaluru, India, in the media, and explore their nature, initiation and propagation using *in situ* observations, and INSAT-3D and INSAT-3DR infrared channel imageries. These gust events occurred on 24 April 2018, 7 and 26 May as well as 2 June 2019. Among these, the 24 April event was the strongest and the instantaneous wind speed exceeded 75 kmph. It is shown that all these cases share some common features. The first is the arrival of a pool of cold air with its minimum temperature that is at least 10 K less compared to what was prevailing about 15 min earlier. The second is the high rainfall rate; 1 min accumulation-based rainfall rate exceeds 100 mm h⁻¹. Extreme winds are short-lived and wind speeds exceeding 50 kmph last for less than 5 min. Satellite imageries of the corresponding period show that the associated clouds were organized with a spatial scale of at least several tens of kilometres.

Keywords: Extreme gust storms, pre-monsoon cold air, satellite imageries.

HIGH-INTENSITY winds over a short duration, popularly known as gusts, are a frequently occurring phenomenon during the summer season¹. India experiences extreme gust storm events during the pre-monsoon months of April and May. These events are localized and not seen in routine synoptic weather charts: however, they cause severe damage to human life, property as well as the environment, and hence to the regional socio-economic conditions². Near the land surface wind speed (generally measured at 10 m height) is normally below 10 m s⁻¹ in a tropical country like India. Higher surface wind speeds are mainly associated with two phenomena. The first is development or passage of an intense synoptic system such as a cyclone. In South Asia, wind extremes are normally associated with tropical cyclones, and the widespread destruction they cause in coastal areas are well

known^{2,3}. Significant progress has been made in recent years in predicting the track and intensity of tropical cyclones at least a few days in advance, giving sufficient time for moving people to safer places^{4,5}. The second source of gust is a cold front driven by a horizontal temperature gradient associated with thunderstorms or dust storms driven by precipitating convective clouds^{6,7}. When precipitation falls through an unsaturated layer of the atmosphere below the cloud base, evaporative cooling generates a cold pool of air which produces a gravity current. The speed of the gravity current (U) is given by^{6,7}

$$U = k \sqrt{gH \frac{T_e - T_c}{T_e}}, \quad (1)$$

where g is the acceleration due to gravity, H the height of the cold pool, T the air temperature, and subscripts c and e refer to cold pool and environment ahead of the cold pool respectively⁷. k is a proportionality constant and reported values range from 0.7 to 1.1 (ref. 7). The lowest temperature that can result due to evaporation in an adiabatic process is the wet bulb temperature. For example, at a temperature of 35°C and relative humidity of 30%, the wet bulb temperature is about 22°C. The actual decrease in surface temperature, however, depends on the initial relative humidity of the sub-cloud layer (downdrafts originating above and reaching the surface can lower the temperature further⁸) and the amount of condensed water that is available for evaporation (which depends on precipitation rate).

The prediction of gust due to a cold pool requires predicting the occurrence of a deep convective cloud/thunderstorm. Predicting the time and location of initiation of deep convective clouds and their propagation remains a grand challenge. Further, majority of thunderstorms do not result in high enough U , i.e. gusts. Therefore, predicting gusts is not trivial. There is also a lack of quantitative information on gusts despite their repeated occurrences each year and associated damages. Physical nature and mechanism of gusts remain unaddressed in the Indian context. This provided the motivation to undertake the present study.

According to media (newspaper) reports, many trees were uprooted and more than 100 electric poles were

*For correspondence. (e-mail: jsatapathy84@gmail.com)

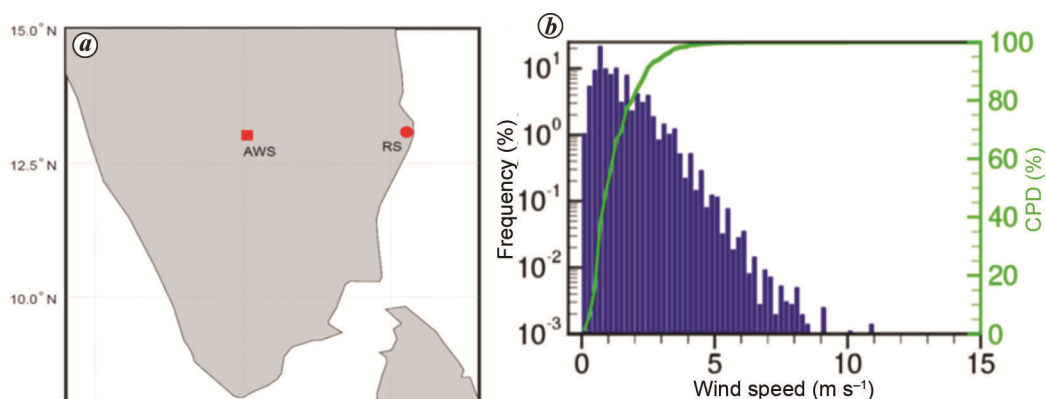


Figure 1. *a*, The automatic weather station (AWS) used in the study is located in the campus of Indian Institute of Sciences, Bengaluru, India (13.02°N, 77.57°E). The nearest upper air station with radiosonde (RS) launch on 24 April 2018 is at Chennai, India (13.08°N, 80.27°E). *b*, Distribution of 10 m height wind speed measured between 1 April and 1 June during 2016–19. Data sampling time interval is 1 min. Bar plot shows the frequency of occurrence, and green coloured line shows the cumulative probability distribution (refer to right axis). Wind speed exceeded 6 and 8.5 m s⁻¹ at 0.1% and 0.01% of the time respectively.

damaged on 24 April 2018 (https://timesofindia.indiatimes.com/city/bengaluru/rain-leaves-residents-in-the-dark-for-24-hours/amp_articleshow/63915898.cms); some areas were without electric power supply for more than two days. The year 2019 also witnessed some cases of damage-causing gust-winds (e.g. 7 and 26 May), where many trees were uprooted/branches fell, resulting in traffic jams and interrupted power supply. Such gust-winds are rare in Bengaluru, Karnataka, India. The present study addresses gust-winds which occurred in Bengaluru in 2018 and 2019. An important finding from this study is that cold pool-driven gust-winds last for a few minutes, and conventional observational systems that normally report average values taken over a time interval of 10 min and longer will not capture the extreme wind intensity.

Data and methods

Gust storms are normally short-lived and last from 1 to 6 h (ref. 9). Therefore, observations with high temporal resolution are needed to analyse the developments leading to the gust event and atmospheric processes associated with it. Here we combine ground observations and satellite data. A 10 m micrometeorological tower is being operated in the campus of the Indian Institute of Science (IISc), Bengaluru (13.02°N 77.57°E; Figure 1*a*). This study uses wind velocity and air temperature data collected using a three-dimensional sonic anemometer (Campbell Scientific Inc., model CSAT3 in 2018 and Gill sonic anemometer, model R3-50 in 2019; both set to sample at 20 Hz). This is supplemented by data collected with an automatic weather station (AWS, Sutron-make) which was installed in June 2015. The AWS wind speed measured with a two-dimensional sonic anemometer (10 m

height), air temperature (T_a) and relative humidity (RH, both measured at 2 m height) and rainfall are archived at 1 min time interval. The ground observations provide information about atmospheric conditions during such extreme events with very high temporal resolution, if the event happens to pass over the measurement location. However, when and where the gust storm is initiated, its temporal evolution, spatial extent and propagation, cannot be understood from a point measurement. The spatial development is as important as the temporal scale in order to understand the physical nature of such short-lived extreme events. In this aspect, geostationary satellite data are useful¹⁰. In particular, Indian geostationary satellites INSAT-3D and INSAT-3DR provide imageries every 30 min. We use brightness temperature (BT) data of the TIR1 channel, viz. 10.95 μm central wavelength (BT11 henceforth) and 3.9 μm (BT4) with a spatial resolution of 4 km at sub-satellite point. The purpose of analysing the satellite data is to know the type of convective cloud system responsible for the gust event¹¹. These data are downloaded from ISRO's MOSDAC site (<https://mosdac.gov.in>) for April and May of 2018 and 2019.

It can be observed from Figure 1*b* that the top 0.01% threshold for wind speed at Bengaluru during April and May is 8.5 m s⁻¹, which is about 30 kmph. Values above the 0.01% bracket would easily qualify as 'extreme events' in climate change studies. A 30 kmph wind speed does not uproot trees or damage man-made structures, and is therefore not considered as extreme for practical purposes. An extreme event is to be seen in the context of the damage it causes, or it should have the potential to cause negative socio-economic impacts¹². Damages to trees and structures start occurring when wind speed touches about 50 kmph or 14 m s⁻¹. In the present study, we have considered only those cases when 1 s average wind speed exceeded 15 m s⁻¹, which occurred on three

days, namely 24 April 2018, 7 and 26 May 2019. All these events are reported to have caused severe damage in Bengaluru. Gust-related damages occurred on 2 June 2019, but not near IISc. This case is also presented.

Results

To gain insight into the physical processes involved in gust events, we start with a detailed case study of the 24 April 2018 event and mention only the salient features of other cases.

The 24 April 2018 case study

AWS data: Figure 2 shows temporal variations measured with the 3D sonic anemometer between 06:00 and 20:00 IST (Indian standard time) on 24 April 2018 at 1 s averaging time interval. Normally, operational AWSs are programmed to provide data at time intervals of 10 min or longer, and for a comparison we have superposed 10 min average values on 1 s average values in the figure. Horizontal wind speed started increasing about 10 min before 14:00 IST, and reached the peak value of more

than 20 m s^{-1} (72 kmph) within the next 15 min (Figure 2a). Wind speeds of more than 15 m s^{-1} lasted for less than 5 min (inset, Figure 2a). In comparison, the peak value of 10 min averaged wind speed is less than 7 m s^{-1} , and the signature of a gust is not at all obvious here. The vertical component of velocity is normally less than 2 m s^{-1} , and exceeded 5 m s^{-1} (18 kmph) during the gust event (Figure 2b). The flow is highly turbulent and transient in nature. The force (drag) exerted by the wind speed is perhaps responsible for uprooting trees, while the intense vertical component for branch felling. Sonic temperature was fluctuating around 30°C before the gust event started; it then decreased below 20°C in the next 15 min and remained nearly unchanged during the next 1 h (Figure 2c). At the instant when the peak in gust was observed, the rainfall rate exceeded 200 mm h^{-1} and this high rate lasted for a few minutes (Figure 2c).

If evaporation of falling raindrops causes cooling, then the moist static energy (MSE, sum of sensible heat, latent heat and potential energy) is conserved¹³. Figure 3a shows the temporal variation of MSE. The MSE reached values $\sim 358 \text{ kJ kg}^{-1}$ by 10:00 IST and remained so till half an hour before the gust arrived; and the decrease in the early afternoon seems to be related to slight drying of the surface layer as seen from the variation of water vapour specific humidity (q , mass of water vapour per unit mass of moist air). When rainfall started, MSE increased

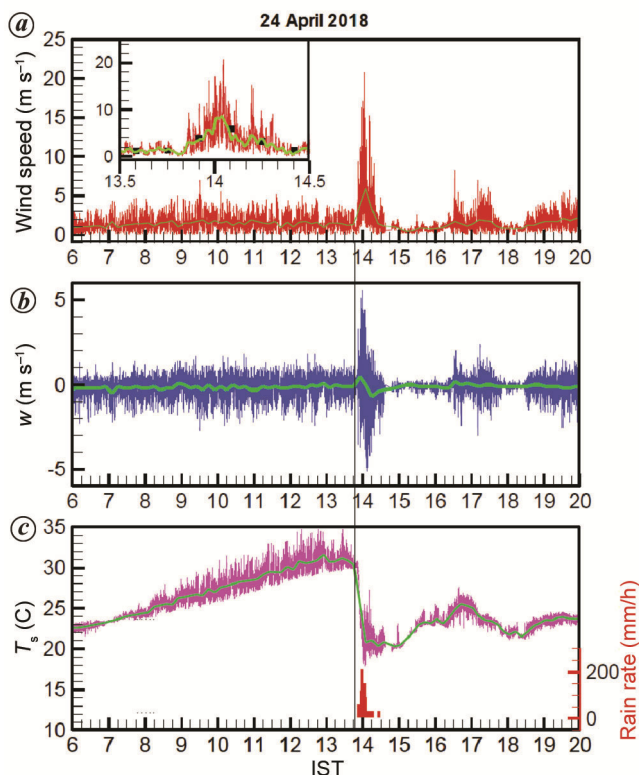


Figure 2. Temporal variations measured at 10 m height with a 3D sonic anemometer on 24 April 2018. **a**, Horizontal component of wind velocity; **b**, vertical component of wind velocity, w ; **c**, temperature (line plot) and rainfall accumulated in 1 min (bar plot, scale on the right axis). Original data are at 20 Hz, and thin and thick green lines refer to averages taken over 1 s and 10 min interval respectively.

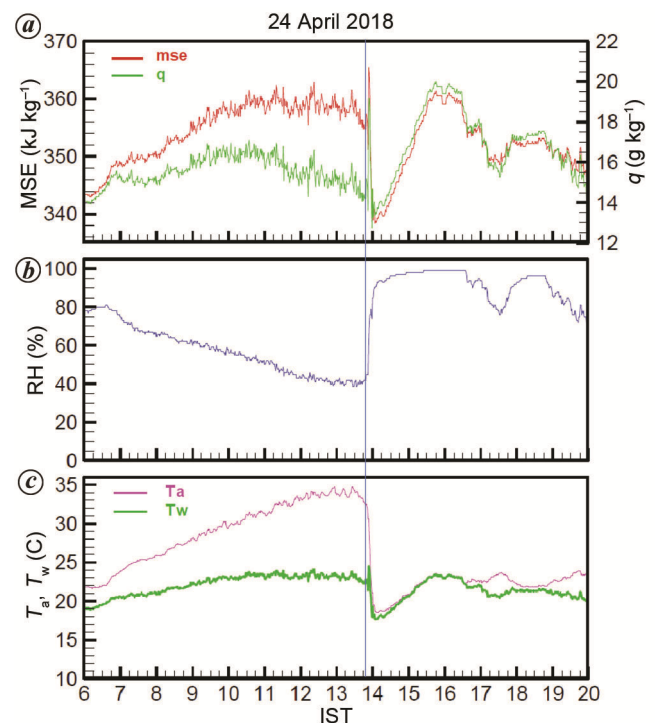


Figure 3. Temporal variation of **(a)** moist static energy (MSE) and specific humidity (q), **(b)** relative humidity (RH) and **(c)** air temperature (T_a) and wet bulb temperature (T_w) observed on 24 April 2018. Data are those of the AWS archived at 1 min time interval. Measurement height is 2 m.

for about 2–3 min (rapid evaporation of raindrops falling on a hot land surface could have increased q and thereby MSE) and then decreased to less than 340 kJ kg^{-1} , which is 15 kJ kg^{-1} less than the pre-gust values. When the rainfall rate is high, falling raindrops can drag air from above to the surface (known as downdraft⁸). The MSE decreases with height in the atmosphere and reaches a minimum around 600 hPa level. The rapid decrease in MSE coinciding with high rainfall rate observed in Figure 3 *a* suggests downdrafts originating from above. To determine the level of origin of downdrafts, high vertical resolution upper air sounding data are required. Although Bengaluru has an upper air sounding station, radiosonde data of 24 April 2018 are not available. The nearest station with sounding data is Chennai (Figure 1 *a*). Figure 4 shows the vertical profiles of MSE and virtual potential temperature (θ_v) based on Chennai radiosonde data. It is seen that MSE decreases below 340 kJ/kg above 1 km height, in the vicinity of the boundary layer top. While Bengaluru and Chennai surface conditions are different, we expect the differences in their thermal properties to be small above the boundary layer since free atmosphere in the tropics is characterized by weak horizontal temperature gradient. Relative humidity increases following rainfall (Figure 3 *b*); a combined effect of decrease in air temperature initially and the subsequent increase in the amount of water vapour. Wet bulb temperature hovered around 21°C before the gust and then dipped further to 17°C

during the intense rainfall, which became possible owing to downdrafts that brought low MSE air from above the boundary layer.

Decrease in air temperature following the diurnal solar cycle is a few degrees Celsius in an hour in the afternoon, and we can expect air ahead of the 24 April gust-front to have a temperature of $\sim 30^\circ\text{C}$. Air temperature inside the cold pool is 17°C , and therefore the temperature difference $\Delta T (=T_e - T_c)$ that drove the gust (see eq. (1)) is $\sim 13^\circ\text{C}$. Such a large ΔT (which is also referred to as cold pool strength in this article) is due to two factors, namely (a) precipitating clouds that developed in the early afternoon when air temperature and RH attain their maximum and minimum values respectively, making the difference between dry and wet bulb temperatures large (Figure 3 *c*), and (b) heavy precipitation which brought dry environmental air from above the boundary layer to the surface and enabled further decrease in the wet bulb temperature compared to the pre-gust conditions.

Satellite data: It is important to understand the physical nature, and both spatial and temporal evolution of the gust from its conception. For this we use INSAT-3D BT11 and BT4 data, and Figure 5 shows the results. BT11, lying in the IR longwave window, senses surface skin temperature in the absence of clouds. Normally, deep convective clouds are identified by low values of BT11 (ref. 14). Figure 5 *a* shows 08:30 UTC BT11 imagery, the nearest image to the time of occurrence of the gust event at the AWS location. Very deep clouds with their BT11 as low as 200 K (corresponding height is $\sim 15 \text{ km}$) are seen near the AWS location. It can be observed from Figure 5 *b* and *c* that deep convective clouds developed suddenly in the area near the AWS, i.e. within 30 min of the gust event, as both 270 and 220 K contours show the absence of clouds extending above the freezing level at 08:00 UTC. Therefore, there were no signs of the possibility of a thunderstorm-driven gust event just half an hour earlier. With time, mid-level clouds represented by 270 K grew larger in size and moved along the southwest–northeast direction, with preference to the southwest. Very deep clouds, on the other hand, do not show such a systematic areal growth or propagation. It can be observed from Figure 5 *a–c* that the AWS was at the edge of a deep convective cloud system with the spatial extent of the cloud defined by the 270 K contour being about 20 km and that by the 220 K threshold only a few kilometres when the gust event occurred. So deep clouds of this event developed almost spontaneously, then propagated southwestward and lasted for more than 2 h. The gust front probably intensified further with time as more cases of destruction were reported in areas lying to the south of IISc. The temporal spread of the 270 K contour suggests a speed of $\sim 40 \text{ kmph}$ in the southwesterly direction.

Figure 5 *d* shows the temporal variations of BT4 and BT11 on 24 April 2018 in the AWS grid. BT11 suggests

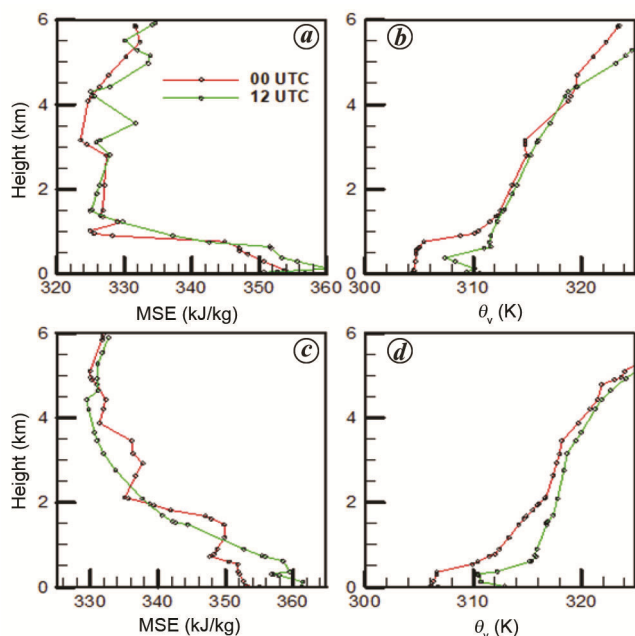


Figure 4. Vertical profiles of MSE (*a*, *c*) and virtual potential temperature (θ_v ; *b*, *d*) based on the radiosonde data of Chennai. *a*, *b*, 24 April 2018. *c*, *d*, 26 May 2019. Rapid increase in θ_v with height is the transition region between the atmospheric mixed layer (boundary layer) and the free atmosphere. The height of this region is approximately that of the atmospheric boundary layer.

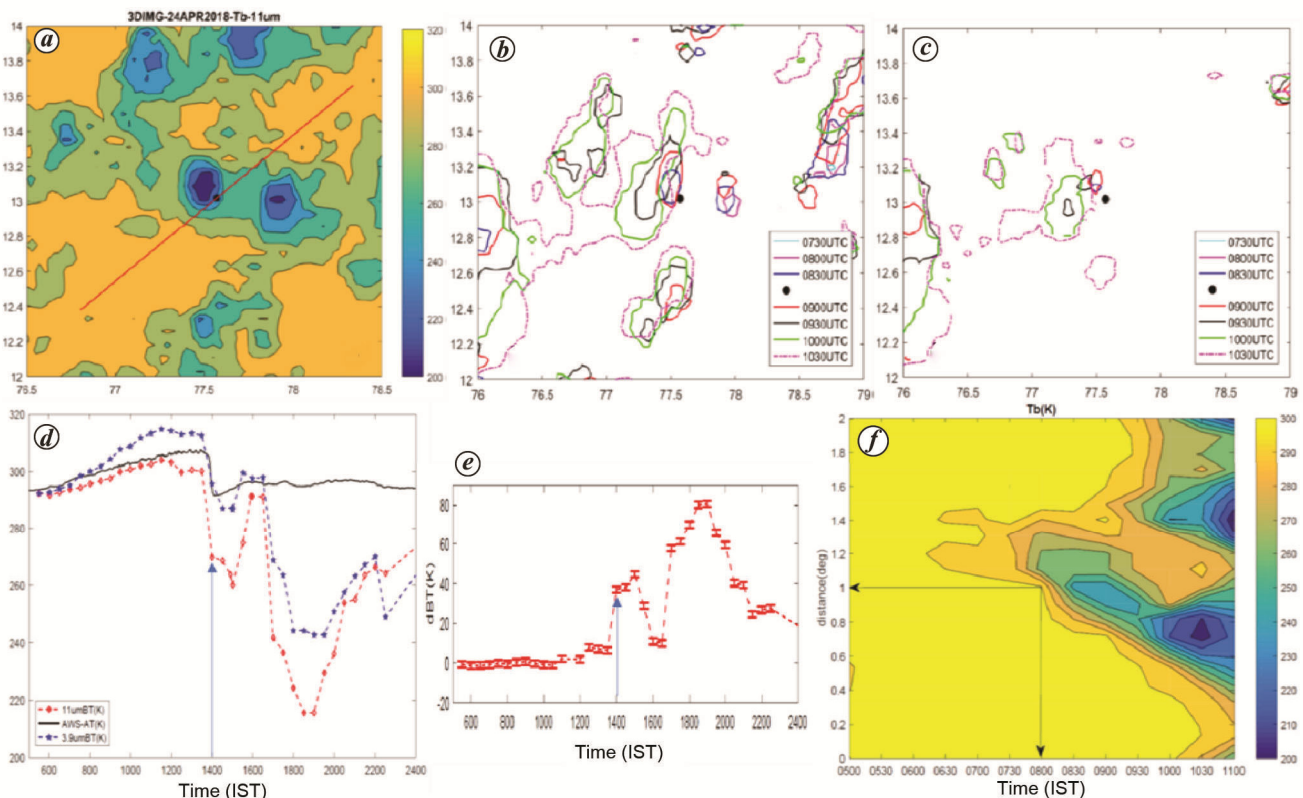


Figure 5. *a*, INSAT-3D brightness temperature BT11 imagery at 08 : 30 UTC on 24 April 2018. The red coloured line is approximately parallel to the direction of growth/propagation of the clouds. The filled circles show the AWS location. *b*, The 270 K contours of BT11 at different times around the gust event. *c*, Contours of 220 K BT11 showing the development of very deep convective clouds. *d*, Temporal variation of BT4 and BT11 in the grid where AWS is located; the AWS-measured air temperature is included for comparison. The arrow indicates the time of the gust event. *e*, Temporal variation of 24 April 2018 BT11 anomaly (dBT) with respect to that for the April month clear sky days. *f*, Temporal variation of BT11 along the straight line shown in (*a*). The distance is measured with respect to A which is at a distance of 1 degree ahead of the AWS.

the development of shallow clouds around noon-time, followed by a rapid vertical development just before 14:00 IST. The deepest clouds were not directly above the AWS, which can also be seen from Figure 5 *a-c*. In order to determine if the temporal evolution of BT11 on the day of the gust event was unusual, we show in Figure 5 *e* the BT11 anomaly (denoted by dBT), calculated with respect to average BT11 of clear sky days in April 2018. Figure 5 *e* suggests that there was nothing unusual about the evolution of BT11 in the morning hours of 24 April 2018. Figure 5 *f* shows the time–distance plot of BT11 along the line shown in Figure 5 *a*. This plot also shows a southwesterly propagation of clouds, and the speed of propagation along the line is ~ 20 kmph ($\sim 0.6^\circ$ distance in 3.5 h). From Figure 5, it can be seen that the gust was associated with a convective system larger than a cumulonimbus cloud, having a size in the meso-beta scale (20–200 km) range¹¹, and is well captured by the 4 km resolution IR data.

The 26 May 2019 case study

AWS data: Figure 6 shows the temporal variation of wind speed, T_a , T_w , mse, q and rainfall on 26 May 2019.

This gust event occurred around 21:00 IST, i.e. at night, and the maximum horizontal wind speed was 19.5 m s^{-1} (70 kmph: Figure 6 *a*). Drop in air temperature compared to what prevailed about 20 min before was 10°C , MSE decreased from 360 to 339 kJ kg^{-1} during this time period, the maximum rainfall rate was 120 mm h^{-1} , and rainfall rate of more than 50 mm h^{-1} prevailed for 19 min. Air temperature was hovering around 35°C at 17:00 IST and decreased to $\sim 28^\circ\text{C}$ by 20:00 IST, by which time the difference between T_a and T_w reduced to 5°C compared to 12°C in the afternoon. Thus, the surface layer had substantially cooled down before the gust arrived, and a 10°C drop in temperature was possible because of downdrafts.

Satellite data: Figure 7 *a* shows the 1515 UTC BT11 imagery, the nearest image to the time of occurrence of the gust event. A deep cloud system of more than 100 km in one direction can be seen approaching the AWS location. This system existed ~ 100 km to the northeast of the AWS at least 2 h earlier, and grew in spatial extent with time as it propagated southwestwards (Figure 7 *b* and *c*). The areal spread of the 270 K contour line of the cloud system suggests an average propagation speed of

~45 kmph in the southwesterly direction. Figure 7d shows the temporal variations of BT4 and BT11 in the grid wherein the AWS lies. BT11 suggests increasing cloud height from 19:30 IST onwards and the lowest value of BT11 is 180 K. Radiosonde data at Bengaluru for 26 May 2019 were not available and so were taken at Chennai and Mangaluru which are the nearest stations; the tropopause height and temperature were about 18 km and -84°C (189 K) respectively. A 180 K value of BT11 suggests that the cumulonimbus clouds were taller than 18 km and penetrated into the stratosphere.

The 7 May 2019 case study

AWS data: AWS measurements revealed that the gust events occurred twice on 7 May (Figure 8). The first event occurred around 15:45 IST, and the maximum wind speed was less than 15 m s^{-1} and the maximum drop in air temperature was about 14°C (Figure 8b). There was some rainfall, but the rate did not exceed 50 mm h^{-1} . Air temperature did not show any major change during the next 3 h and wind speed reduced below 1 m s^{-1} by 19:00 IST. Then the winds picked up, reaching more than 17 m s^{-1} around 19:30 IST. Since the surface layer temperature

was already low due to the first gust event, air was nearly saturated and drop in air temperature during the second event was only a few degrees Celsius. Therefore, the high winds are not of cold-pool origin. The peak rainfall rate was high (180 mm h^{-1}) (Figure 8b), and MSE decreased by 8 kJ kg^{-1} . Therefore, there was downdraft, and heavy precipitation also brought air having higher wind speed/momentum from above to the surface. Since wind data above 10 m were not available, it is not certain at what height high wind speeds prevailed. The second gust event of 7 May suggests that downdrafts not only brought low MSE air from above, but higher momentum as well.

Satellite data: Figure 9a shows the 10:30 UTC BT11 imagery, the nearest image to the time of occurrence of the gust event. Deep convective clouds were present to the north of the AWS, while those directly above the AWS were warm clouds (i.e. cloud top below the freezing level; Figure 9b and c). A larger and deeper cloud system existed to the east and northeast of the AWS, which propagated westward and moved over the AWS grid around 17:00 IST. Rainfall did not occur at this time (Figure 8b), suggesting that the deep cloud cover was probably a westward-spreading outflow of cumulonimbus clouds that developed some distance away. When the second gust event occurred, very deep clouds with BT11 less than 200 K were present and this also corroborates with very high rainfall rates measured around the same time (Figure 8b). The temporal variation of the contours indicates a propagation speed of $\sim 30\text{ kmph}$ for the deep cloud cover spread.

Figure 9d, showing the temporal variations of BT4 and BT11 on 7 May 2019 in the AWS grid suggests the development of deep convective clouds $\sim 2\text{ h}$ before the occurrence of rainfall at the AWS location. Figure 9e showing two peaks for dBT also suggests the initial development of shallow convective activity followed by deep convective activity. The 14:00 UTC BT11 imagery shows a north–south-oriented deep convective cloud system around the time when the second gust event occurred (Figure 9f). Its spatial pattern (extent is more than 200 km normal to the direction of propagation, while $\sim 50\text{ km}$ along the direction) suggests that it was a squall line⁹.

The 2 June 2019 case study

Fallen trees and broken electric poles were reported in Bengaluru on 2 June 2019. The deep cloud cover was extensive over the city around that time (Figure 10a). The maximum wind speed measured in the IISc campus was less than 11 m s^{-1} (Figure 11a), cold-pool strength was $\sim 6^{\circ}\text{C}$ (air temperature decreased from 28°C to 22°C in 30 min; Figure 11b), and maximum rainfall rate was

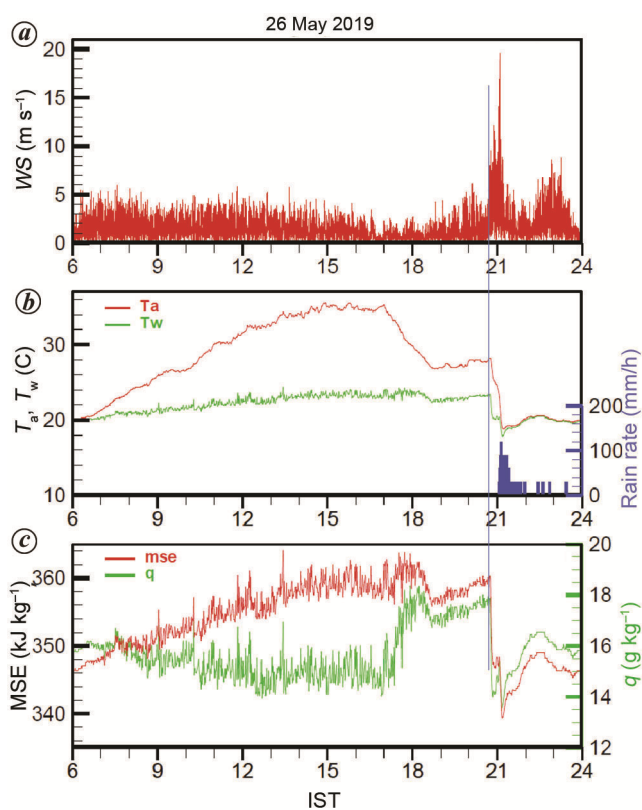


Figure 6. Temporal variations observed on 26 May 2019. *a*, Horizontal component of wind speed (1 s average) measured with Gill sonic anemometer. *b*, Air temperature and wet bulb temperature, as well as rain rate (bar plot). *c*, Plot of MSE and specific humidity.

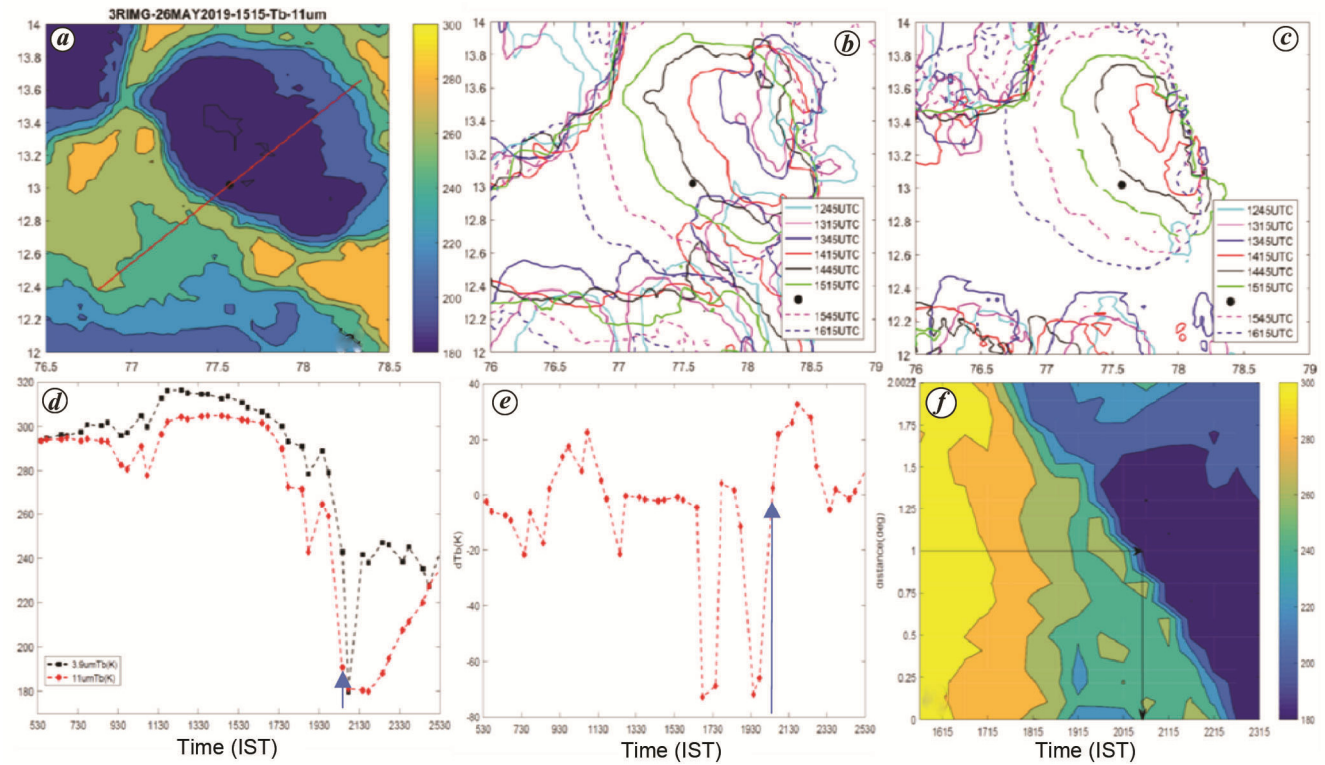


Figure 7. Same as Figure 5, but for 26 May 2019.

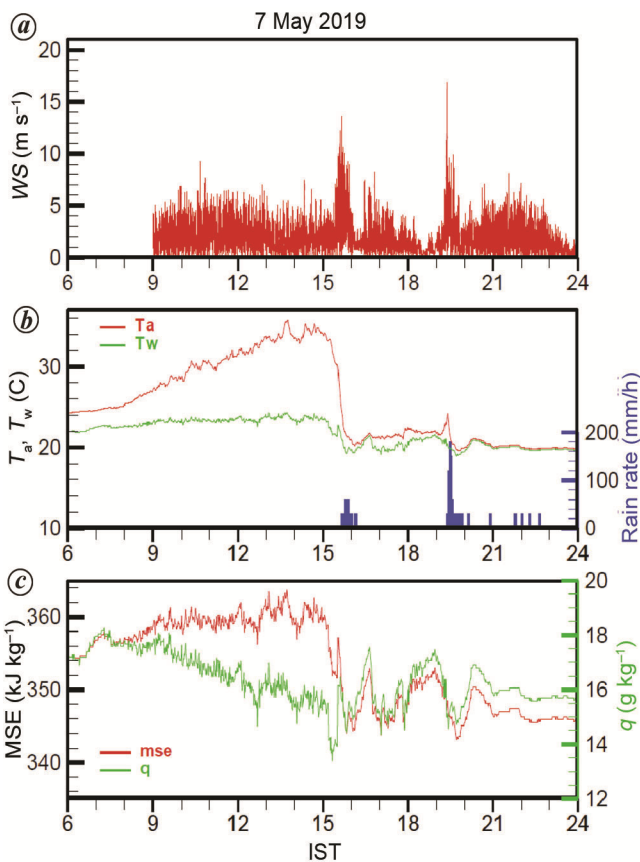


Figure 8. Same as Figure 6, but for 7 May 2019.

less than 100 mm h^{-1} . Thus, the AWS was not in the path of the gust on that day.

Discussion

In eq. (1), U depends on two variables, namely H and ΔT . Since the coldest air descends to the surface, ΔT driving the gravity current is well represented by the AWS-measured temperature. It is of interest to determine how the maximum wind speed at 10 m height varies with ΔT . Figure 12 shows a scatter plot of ΔT versus maximum wind speed using the AWS data of four April to May time periods. The maximum change in air temperature and maximum wind speed in a 20 min window were obtained and only those cases with $\Delta T \geq 6^\circ\text{C}$ were plotted. Figure 12 highlights that the correlation between ΔT and maximum wind speed is poor; variations in H may be one of the reasons. Second, the number of instances when $\Delta T \geq 10^\circ\text{C}$ is 1, 2, 3 and 6 during 2016, 2017, 2018 and 2019 respectively, and all cases with wind speed $>10 \text{ m s}^{-1}$ occurred in 2018 and 2019.

An important aspect that emerges from the case studies is that maximum gust nearly coincides with the peak in rainfall rate (typically more than 100 mm h^{-1}). The lowest values of MSE are observed around this time, i.e. downdraft originating from above the boundary layer reaches the surface (in a well-mixed atmosphere, MSE is nearly constant with height). Due to ground friction, wind slows

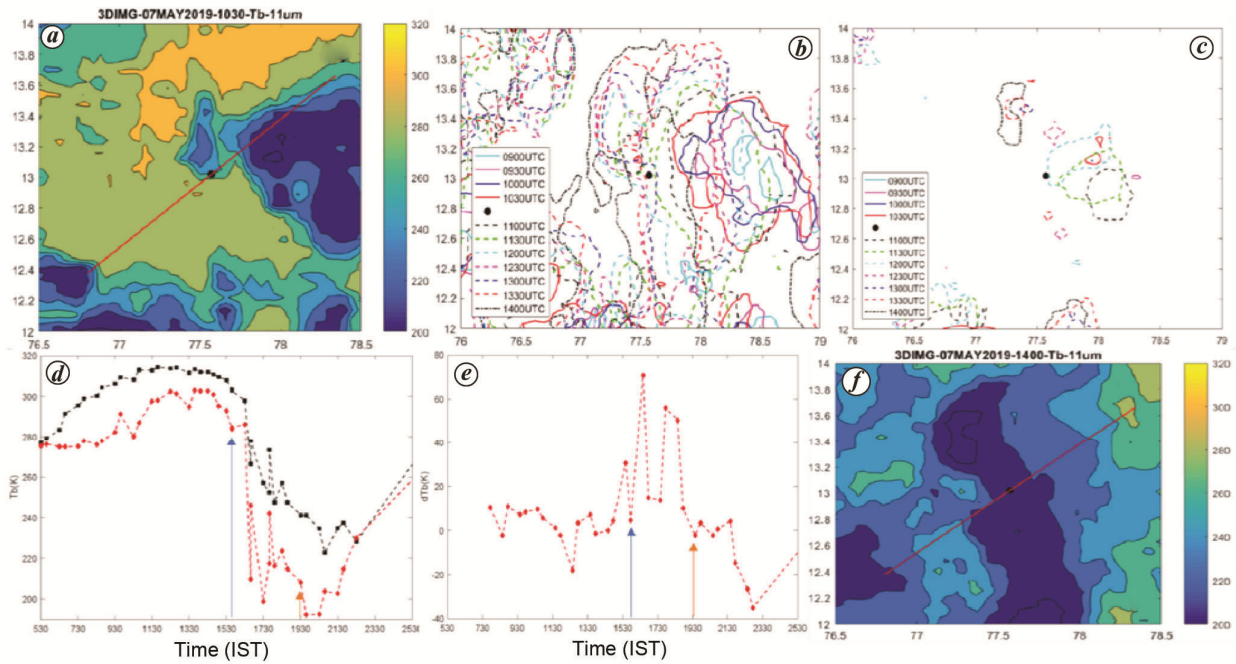


Figure 9. Same as Figure 5 but for 7 May 2019. Here (f) shows BT11 imagery at 14:00 UTC, the nearest image to the second gust event.

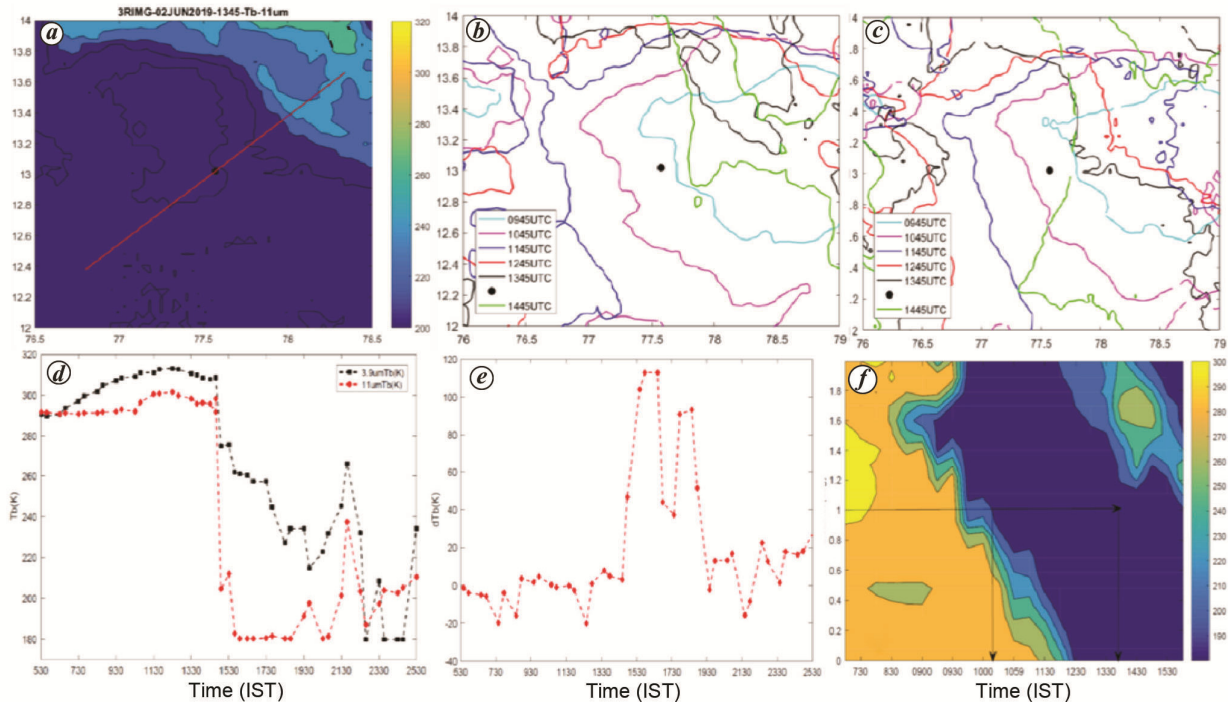


Figure 10. Same as Figure 5, but for 2 June 2019.

down near the surface but rapidly increases with height. Maximum gusts occur a few hundred metres above the surface in a cold pool-driven wind system in the atmosphere⁷. Summer-time thunderstorms produce both cold pool and downdrafts, and high winds from above are brought down to the surface by the downdrafts. This is the reason why most intense gusts and rainfall rates occur simultaneously.

Concluding remarks

This study emphasizes on the understanding of the physical nature of extreme gust events of different characteristics based on four case studies using ground observations and INSAT-3D/3DR data, which in future can be helpful in now casting of extreme events. Gusts being short-lived demand observations made with high temporal resolution.

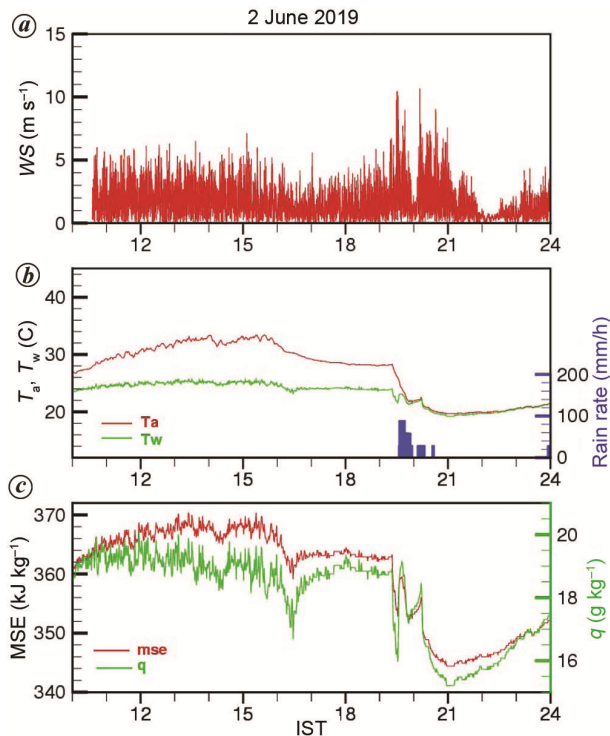


Figure 11. Same as Figure 6, but for 2 June 2019.

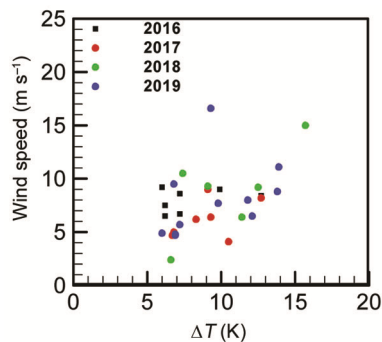


Figure 12. Scatter plot of maximum temperature change (ΔT) versus maximum wind speed measured in a 15 min interval time window. Values when $\Delta T \geq 6$ K are only plotted. AWS data archived at 1 min time interval for 2016–19 are used.

Observations of INSAT-3D and INSAT-3DR, with 30 min temporal resolution have been useful to study the origin of gust storms, temporal evolution and propagation. Temperature gradient, spatial extent and speed of the gust systems have been deciphered from IR brightness temperatures. The meteorological parameters, viz. air temperature, humidity, rainfall, wind speed and moist static energy from sonic anemometers and AWS measurements at IISc have also been considered here to gain insights.

Our important findings are as follows:

- Pre-monsoon gust events over Bengaluru are either driven by a cold pool or by strong downdrafts driven by intense precipitation from a deep convective cloud, or both.

- Gust events render short-term perturbation in the atmospheric thermodynamic properties, especially in the boundary layer in terms of turbulent mixing, lowering the MSE, high rainfall rates, sudden decrease in air temperature and increase in relative humidity.
- Temperature signatures of gust storms as captured by brightness temperature of longwave IR window channel show that there is a significant temperature gradient just ahead of the gust event.
- All four convective systems that produced gusts in Bengaluru during the pre-monsoon season propagated westward or southwestward with speeds of 20–50 kmph.

1. Brasseur, O., Development and application of a physical approach to estimating wind gusts. *Mon. Wea. Rev.*, 2001, **129**, 5–25.
2. Rauber, R., Walsh, J. and Charlevoix, D., *Severe and Hazardous Weather*, Kendall Hunt, 2002, p. 616.
3. Mohapatra, M. and Sharma, M., Cyclone warning services in India during recent years: a review. *Mausam*, 2019, **70**, 635–666.
4. Mohapatra, M., Geetha, B. and Sharma, M., Reduction in uncertainty in tropical cyclone track forecasts over the North Indian Ocean. *Curr. Sci.*, 2017, **112**, 1826–1830.
5. Landsea, C. W. and Cangialosi, J. P., Have we reached the limits of predictability for tropical cyclone track forecasting? *Bull. Am. Meteorol. Soc.*, 2018, **99**, 2237–2243.
6. Wakimoto, R. M., The life cycle of thunderstorm gust fronts as viewed with Doppler radar and rawinsonde data. *Mon. Wea. Rev.*, 1982, **110**, 1060–1082.
7. Droegemeier, K. K. and Wilhelmson, R. B., Numerical simulation of Thunderstorm outflow dynamics. Part I: outflow sensitivity experiments and turbulence dynamics. *J. Atm. Sci.*, 1987, **44**, 1180–1210.
8. Knupp, K. R. and Cotton, W. R., Convective cloud downdraft structure: an interpretive survey. *Rev. GeoPhys.*, 1985, **23**, 183–215.
9. Houze Jr, R. A., *Cloud Dynamics*, Academic Press, San Diego, 1993, p. 573.
10. Satapathy, J. and Jangid, B. P., Monitoring a local extreme weather event with the scope of hyperspectral sounding. *Meteorol. Atmos. Phys.*, 2018, **130**, 371–381.
11. Orlanski, I., A rational subdivision of scales for atmospheric processes. *Bull. Am. Meteorol. Soc.*, 1975, **56**, 527–530.
12. WMO, *Guidelines on the Definition and Monitoring of Extreme Weather and Climate Events*, WMO Commission for Climatology Task Team on the Definition of Extreme Weather and Climate Events, 2018.
13. Iribarne, J. V. and Godson, W. L., *Atmospheric Thermodynamics*, D. Reidel Publishing Company, Dordrecht, Holland, 1973.
14. Ackerman, S. A. *et al.*, Discriminating clear sky from clouds with MODIS. *J. Geophys. Res.*, 1998, **103**, 32141–32157.

ACKNOWLEDGEMENTS. The 3D sonic anemometers used in this study were procured as part of INCOMPASS and CTCZ programmes funded by the Ministry of Earth Sciences, Government of India. Major part of this study was carried out when the first author visited IISc in 2019, which was supported by the National Science Academies' Summer Research Fellowship Programme for Teachers. We thank MOSDAC-ISRO for making freely available INSAT-3D and INSAT-3DR data, and India Meteorological Department for the Chennai radiosonde data.

Received 18 July 2019; accepted 23 April 2020

doi: 10.18520/cs/v119/i2/343-351